Interference-induced gain in the Autler-Townes doublet of a V-type atom in a cavity

Peng Zhou,[1,*] S. Swain,[2] and L. You[1]
[1]*School of Physics, Georgia Institute of Technology, Atlanta, Georgia 30332-0430*
[2]*Department of Applied Mathematics and Theoretical Physics, The Queen's University of Belfast, Belfast BT7 1NN, United Kingdom*
(Received 5 July 2000; published 15 February 2001)

We study the Autler-Townes spectrum of a V-type atom coupled to a single-mode, frequency-tunable cavity field at finite temperature, with a pre-selected polarization in the bad cavity limit, and show that, when the mean number of thermal photons $N \gg 1$ and the excited sublevel splitting is very large (of the same order as the cavity linewidth), probe gain may occur at either sideband of the doublet, depending on the cavity frequency, due to cavity-induced quantum interference. It is also possible to choose the cavity detuning so that one of the Autler-Townes sidebands vanishes.

DOI: 10.1103/PhysRevA.63.033818 PACS number(s): 42.50.Gy, 42.50.Ct, 32.80.−t, 03.65.−w

In recent years, there has been a resurgence of interest in the phenomenon of quantum interference [1]. It provides the origin of many new effects and applications of quantum optics, such as lasing without population inversion [2], electromagnetically induced transparency [3], enhancement of the index of refraction without absorption [4], fluorescence quenching [5–8], and spectral line narrowing [6,9].

The basic system consists of a singlet state connected to a closely spaced excited doublet by a single-mode laser. Cardimona *et al.* [5,6] studied the effect of quantum interference on the resonance fluorescence of such a system, and found that it can be driven into a dark state in which quantum interference prevents any fluorescence from the excited sublevels, regardless of the intensity of the exciting laser. We have recently shown that quantum interference can also lead to narrow resonances, transparency, and gain without population inversion in the probe absorption spectrum of such an atomic system [10].

Harris and co-workers [2] generalized the V-type atom to systems where the excited doublets decay to an additional continuum or to a single auxiliary level, in addition to the ground state. They found that at a certain frequency the absorption rate goes to zero due to destructive interference whereas the emission rate remains finite. It is possible to amplify a laser field at this frequency without population inversion being present. In the case of a single auxiliary level, quantum interference can lead to the elimination of the spectral line at the driving laser frequency in the spontaneous emission spectrum [7] and transparency in the absorption spectrum [11].

An experimental investigation of interference-induced suppression of spontaneous emission was carried out in sodium dimers, where the excited sublevels are superpositions of singlet and triplet states that are mixed by a spin-orbit interaction [8,12]. A subsequent experiment failed to observe the same features [13]. A detailed theoretical investigation of this system has recently been provided, which found that the number of peaks in the spectrum depends upon the excitation process [14].

It is important for all these effects that the dipole moments of the transitions involved are parallel, or very nearly so, so that the *cross-decay terms* are maximal. In practice, however, it is difficult to find isolated atomic systems that have parallel moments [2,5,12,17]. Various alternative proposals [15,17,18] have been made for generating quantum interference effects. For example, if the two upper levels of a V-type atom are coupled by a microwave field or an applied laser, the excited doublet becomes a superposition, so that as the atom decays from one of the excited sublevels it drives the other. For such systems, cross-decay terms are evident in the atomic dressed picture [15]. The experimental observation of destructive interference between the transition probability amplitudes from the ground state to the excited doublets (dressed states) in terms of electromagnetically induced transparency has been reported in many laboratories [3,16].

Patnaik and Agarwal have shown that the effect of quantum interference can also occur in a four-level atom with two closely spaced intermediate states coupled to a two-mode cavity with preselected polarizations [17]. Recently, Agarwal [18] has proposed a scheme whereby quantum interference can be produced by the anisotropy of the electromagnetic vacuum, for closely spaced states. A cavity could naturally provide the implementation of the proposal [18].

We have recently also proposed a scheme for the engineering of quantum interference (the production of parallel or antiparallel dipole moments) in a V-type atom coupled to a frequency-tunable, single-mode cavity field with a preselected polarization at zero temperature [19]. We have found that the effects of the cavity-induced interference are pronounced only when the cavity detuning δ and the excited doublet splitting ω_{21} are much less than the cavity linewidth 2κ. Here we shall extend the study to a cavity damped by a *thermal reservoir* at finite temperature, so that the mean number of thermal photons N in the cavity mode is nonzero. We show that, even in the case when δ and ω_{21} are of the same order as the cavity linewidth 2κ, the cavity-induced interference is still significant when $N \gg 1$, and that interference-assisted gain may occur in one component of the Autler-Townes doublet for a certain cavity resonant frequency. Such interference-related gain in the Autler-Townes doublet is also reported in free space [20]. We note that Ref. [20] presented a scheme for detecting the quantum interfer-

*Electronic address: peng.zhou@physics.gatech.edu

 ©2001 The American Physical Society

ence resulting from nonorthogonally oriented dipole transitions in free space, by a sophisticated arrangement of the pump and probe lasers, rather than for generating quantum interference.

Our model consists of a V-type atom with the ground state $|0\rangle$ coupled by the single-mode cavity field to the excited doublet $|1\rangle,|2\rangle$. Direct transitions between the excited sublevels $|1\rangle$ and $|2\rangle$ are dipole forbidden. The master equation for the total density matrix operator ρ_T in the frame rotating with the average atomic transition frequency $\omega_0 = (\omega_{10}+\omega_{20})/2$ takes the form

$$\dot{\rho}_T = -i[H_A + H_C + H_I, \rho_T] + \mathcal{L}\rho_T, \tag{1}$$

where

$$H_C = \delta a^\dagger a, \tag{2a}$$

$$H_A = \frac{1}{2}\omega_{21}(A_{22} - A_{11}), \tag{2b}$$

$$H_I = i(g_1 A_{01} + g_2 A_{02})a^\dagger - \text{H.c.}, \tag{2c}$$

$$\mathcal{L}\rho_T = \kappa(N+1)(2a\rho_T a^\dagger - a^\dagger a\rho_T - \rho_T a^\dagger a) + \kappa N(2a^\dagger \rho_T a - aa^\dagger \rho_T - \rho_T aa^\dagger) \tag{2d}$$

with

$$\delta = \omega_C - \omega_0, \quad \omega_{21} = E_2 - E_1,$$

$$g_i = \mathbf{e}_\lambda \cdot \mathbf{d}_{0i}\sqrt{\frac{\hbar\omega_C}{2\epsilon_0 V}} \quad (i=1,2). \tag{3}$$

Here H_C, H_A, and H_I are the unperturbed cavity, the unperturbed atom, and the cavity-atom interaction Hamiltonians, respectively, while $\mathcal{L}\rho_T$ describes damping of the cavity field by the continuum electromagnetic modes at finite temperature, characterized by the decay constant κ and the mean number of thermal photons N; a and $a^\dagger$ are the photon annihilation and creation operators of the cavity mode, and $A_{ij} = |i\rangle\langle j|$ is the atomic population (the dipole transition) operator for $i=j$ $(i\neq j)$; δ is the cavity detuning from the average atomic transition frequency, ω_{21} is the splitting of the excited doublet of the atom, and g_i is the atom-cavity coupling constant, expressed in terms of $\mathbf{d}_{ij}$, the dipole moment of the atomic transition from $|j\rangle$ to $|i\rangle$, $\mathbf{e}_\lambda$, the polarization of the cavity mode, and V, the volume of the system. For simplicity, we assume here that the atomic spontaneous decay through the sides of the cavity can be neglected. In the remainder of this work we assume that the polarization of the cavity field is *preselected*, i.e., the polarization index λ is fixed to one of two possible directions.

In this paper we are interested in the bad cavity limit $\kappa \gg g_i$, that is, the atom-cavity coupling is weak, and the cavity has a low Q so that the cavity field decay dominates. The cavity field response to the continuum modes is much faster than that produced by its interaction with the atom, so that the atom always experiences the cavity mode in the state induced by the thermal reservoir. Thus one can adiabatically eliminate the cavity-mode variables, giving rise to a master equation for the atomic variables only [21], which takes the form

$$\begin{aligned}\dot{\rho} = &-i[H_A,\rho] + \{F(\omega_{21})(N+1)[|g_1|^2(A_{01}\rho A_{10} - A_{11}\rho) \\ &+ g_1 g_2^*(A_{01}\rho A_{20} - A_{21}\rho)] + F(-\omega_{21})(N+1) \\ &\times[|g_2|^2(A_{02}\rho A_{20} - A_{22}\rho) + g_1^* g_2(A_{02}\rho A_{10} - A_{12}\rho)] \\ &+ F(\omega_{21})N[|g_1|^2(A_{10}\rho A_{01} - \rho A_{00}) + g_1 g_2^* A_{20}\rho A_{01}] \\ &+ F(-\omega_{21})N[|g_2|^2(A_{20}\rho A_{02} - \rho A_{00}) + g_1^* g_2 A_{10}\rho A_{02}] \\ &+ \text{H.c.}\},\end{aligned} \tag{4}$$

where $F(\pm\omega_{21}) = [\kappa + i(\delta \pm \omega_{21}/2)]^{-1}$.

Obviously, Eq. (4) describes cavity-induced atomic decay into the cavity mode. The real part of $F(\pm\omega_{21})|g_j|^2$ represents the cavity-induced decay rate of the atomic excited level $j(=1,2)$, while the imaginary part is associated with the frequency shift of the atomic level resulting from the interaction with the vacuum field in the detuned cavity. The other terms, $F(\pm\omega_{21})g_i g_j^*$, $(i\neq j)$, however, represent cavity-induced correlated transitions of the atom, i.e., an emission followed by an absorption of the same photon on a different transition, $(|1\rangle\rightarrow|0\rangle\rightarrow|2\rangle$ or $|2\rangle\rightarrow|0\rangle\rightarrow|1\rangle)$, which give rise to the effect of quantum interference.

The effect of quantum interference is very sensitive to the orientations of the atomic dipoles and the polarization of the cavity mode. For instance, if the cavity-field polarization is not preselected, as in free space, one must replace $g_i g_j^*$ by the sum over the two possible polarization directions, giving $\Sigma_\lambda g_i g_j^* \propto \mathbf{d}_{0i}\cdot\mathbf{d}_{0j}^*$ [17]. Therefore, only nonorthogonal dipole transitions lead to nonzero contributions, and the maximal interference effect occurs with the two dipoles parallel. As pointed out in Refs. [2,5,17,12], however, it is questionable whether there is an isolated atomic system with parallel dipoles. Otherwise, if the polarization of the cavity mode is fixed, say $\mathbf{e}_\lambda = \mathbf{e}_x$, the polarization direction along the x quantization axis, then $g_i g_j^* \propto (\mathbf{d}_{0i})_x(\mathbf{d}_{0j}^*)_x$, which is nonvanishing, regardless of the orientation of the atomic dipole matrix elements.

It is apparent that if $\kappa \gg \delta$, ω_{21}, the frequency shifts are negligibly small [19], and thus Eq. (4) reduces to that of a V-type atom with two parallel transition matrix elements in free space [5,6,10]. In the following we shall discuss the effect of quantum interference by examining this system's steady-state absorption spectrum, which is defined as

$$A(\omega) = \text{Re}\int_0^\infty \lim_{t\rightarrow\infty}\langle[P(t+\tau), P^\dagger(t)]\rangle e^{i\omega\tau}d\tau, \tag{5}$$

where $\omega = \omega_p - \omega_0$, ω_p being the frequency of the probe field, and $P(t) = d_1 A_{01} + d_2 A_{02}$ is the component of the atomic polarization operator in the direction of the probe field polarization vector $\mathbf{e}_p$, with $d_i = \mathbf{e}_p\cdot\mathbf{d}_{0i}$. With the help of the quantum regression theorem, one can calculate the spectrum from the Bloch equations

$$\langle \dot{A}_{11}\rangle = -[F(\omega_{21})+F^*(\omega_{21})]|g_1|^2[(N+1)\langle A_{11}\rangle - N\langle A_{00}\rangle] - F(-\omega_{21})g_1^* g_2(N+1)\langle A_{12}\rangle - F^*(-\omega_{21})g_1 g_2^*(N+1)\langle A_{21}\rangle,$$

$$\langle \dot{A}_{22}\rangle = -[F(-\omega_{21})+F^*(-\omega_{21})]|g_2|^2[(N+1)\langle A_{22}\rangle - N\langle A_{00}\rangle] - F^*(\omega_{21})g_1^* g_2(N+1)\langle A_{12}\rangle - F(\omega_{21})g_1 g_2^*(N+1)\langle A_{21}\rangle,$$

$$\langle \dot{A}_{12}\rangle = -F(\omega_{21})g_1 g_2^*(N+1)\langle A_{11}\rangle - F^*(-\omega_{21})g_1 g_2^*(N+1)\langle A_{22}\rangle + [F(\omega_{21})+F^*(-\omega_{21})]g_1 g_2^* N\langle A_{00}\rangle - [F^*(\omega_{21})|g_1|^2(N+1)+F(-\omega_{21})|g_2|^2(N+1) + i\omega_{21}]\langle A_{12}\rangle,$$

$$\langle \dot{A}_{01}\rangle = -\left[F(\omega_{21})|g_1|^2(2N+1)+F(-\omega_{21})|g_2|^2 N - i\frac{\omega_{21}}{2}\right]\times\langle A_{01}\rangle - F(-\omega_{21})g_1^* g_2(N+1)\langle A_{02}\rangle,$$

$$\langle \dot{A}_{02}\rangle = -\left[F(\omega_{21})|g_1|^2 N+F(-\omega_{21})|g_2|^2(2N+1)+i\frac{\omega_{21}}{2}\right]\times\langle A_{02}\rangle - F(\omega_{21})g_1 g_2^*(N+1)\langle A_{01}\rangle. \quad (6)$$

To monitor quantum interference, we insert a factor η $(=0,1)$ in the cross-transition terms $g_i g_j^*$. When $\eta=0$, the cross transitions are switched off, so no quantum interference is present. Otherwise, the effect of quantum interference is maximal.

It will be shown that for dominant quantum interference effects we need to work in the region $\omega_{21}\geqslant\kappa$ and $N\gg 1$. Physically, the incoherent thermal reservoir plays the role of a driving field here, and the condition $N\gg 1$ ensures that the stimulated and spontaneous decay rates are approximately equal. The condition $\omega_{21}\geqslant\kappa$ means that the cavity mode can couple to the two transition channels. The detuning δ can vary over a very wide range and the spectra still show interesting features, as the following figures illustrate. However, in the limit $\delta\gg\omega_{21}$, the effects of quantum interference vanish.

Figure 1 shows the Autler-Townes spectra for $g_1=g_2=10$, $\kappa=\omega_{21}=100$, $N=10$, and different cavity detunings. In the absence of interference $(\eta=0)$, the two transition paths $|0\rangle\leftrightarrow|1\rangle$ and $|0\rangle\leftrightarrow|2\rangle$ are *independent*. These transitions lead to the lower and higher frequency sidebands of the absorption doublet, respectively. It is not difficult to see that the spectral heights and linewidths are mainly determined by the cavity-induced decay constants $\gamma_i(i=1,2)$ of the excited states, which have the forms

$$\gamma_1=\frac{\kappa|g_1|^2}{\kappa^2+(\delta+\omega_{21}/2)^2},\quad \gamma_2=\frac{\kappa|g_2|^2}{\kappa^2+(\delta-\omega_{21}/2)^2}, \quad (7)$$

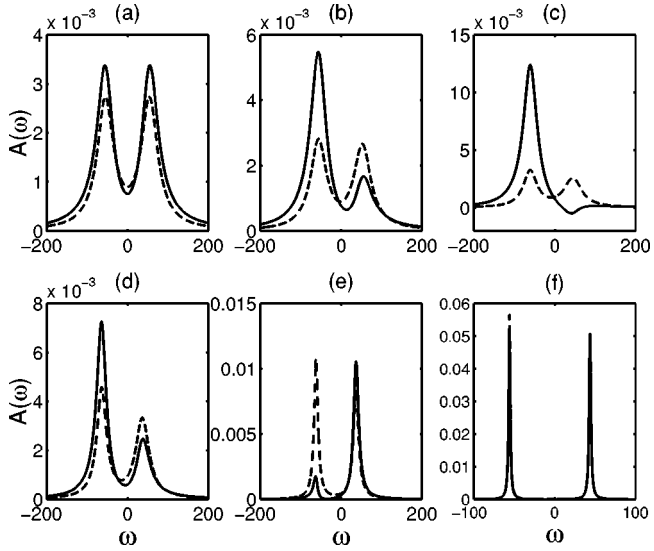

FIG. 1. Absorption spectrum for $g_1=g_2=10$, $\kappa=100$, $\omega_{21}=100$, $N=10$, and $\delta=0$, 10, 50, 100, 200, 500 in (a)–(f), respectively. In Figs. 1–3 the solid curves represent the spectrum in the presence of the maximal interference $(\eta=1)$, while the dashed curves are the spectrum in the absence of the interference $(\eta=0)$.

and depend on the cavity frequency. It is evident that $\gamma_1<\gamma_2$ when $\delta>0$, and both γ_1 and γ_2 decrease as δ increases. Noting that the lower and higher frequency peaks have linewidths $\Gamma_l=\gamma_1(2N+1)+\gamma_2 N$ and $\Gamma_h=\gamma_1 N+\gamma_2(2N+1)$, and have heights proportional to $\Gamma_{l,h}^{-1}$, the lower frequency sideband is slightly higher than the higher frequency one for $\delta>0$ and both sidebands can be narrowed by increasing the cavity detuning. See, for example, the dashed lines in the following three figures.

The spectral features are dramatically modified in the presence of the cavity-induced interference $(\eta=1)$. When the cavity is resonant with the average frequency of the atomic transitions, $\delta=0$, the doublet is symmetric, and its sidebands are higher and wider than that for $\eta=0$, as shown in Figs. 1(a), 2(a), and 3(a). Otherwise, it is asymmetric. Either sideband of the doublet can be suppressed, depending upon the cavity frequency, e.g., the higher frequency sideband is suppressed for $\delta=10$, 50, and 100, see in Figs. 1(b)–1(d), while the sideband is enhanced for $\delta=200$, shown in Fig. 1(e). When the cavity frequency is far off resonant with the atomic transition frequencies, say $\delta=500$ as in Fig. 1(f), the absorption spectra for $\eta=0$ and 1 are virtually the same, that is, the effect of cavity-induced interference is negligible small.

Rather surprisingly, Fig. 1(c) shows probe gain in the higher frequency sideband, without the help of any coherent pumping. Moreover, increasing the mean number of thermal photons N may enhance the probe gain; see, for instance, Fig. 2 for $N=20$, in which higher frequency probe gain even occurs for a relatively small cavity detuning, such as $\delta=10$ in Fig. 2(b). By contrast, when the detuning is very large, the probe beam can be amplified at the lower frequency sideband, rather than at the higher frequency one, as shown in

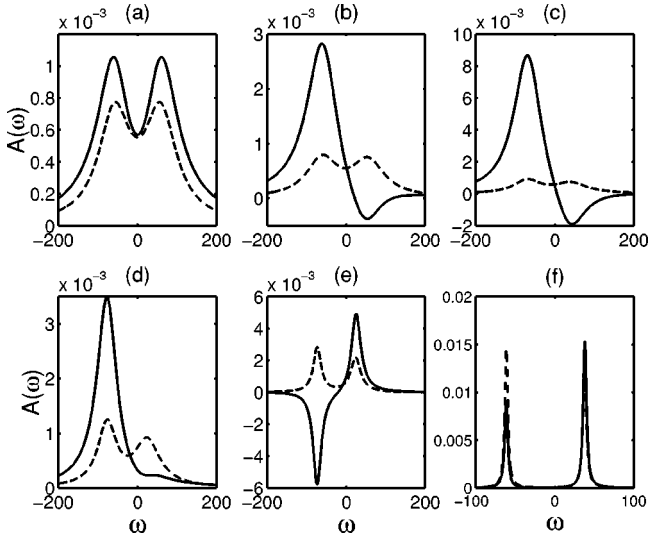

FIG. 2. Same as Fig. 1, but with $N=20$.

Fig. 2(e) for $\delta=200$, for example. Figure 2 also shows that the linewidths are broadened for a large number of thermal photons.

In Fig. 3, we present the Autler-Townes spectrum for a large excited level splitting, $\omega_{21}=200$, and a large number of thermal photons, $N=20$. We find that more pronounced gain, as compared with that for $\omega_{21}=100$, is displayed at the lower frequency sideband for $\delta=10$, 50, and 100, and at the higher frequency sideband for $\delta=200$. One also finds that for the larger level splitting the effect of the cavity-induced interference is still significant when $\delta=500$, as shown in Fig. 3(f), where the lower frequency peak is almost suppressed while the higher is greatly enhanced. However, when $\delta \gg \omega_{21}$, say for $\delta=1000$, the effect of the interference disappears. (We have presented no figure here.)

In what follows, we shall see that the probe gain is a direct consequence of the cavity-induced quantum interference between the two transition paths $|0\rangle \leftrightarrow |1\rangle$ and

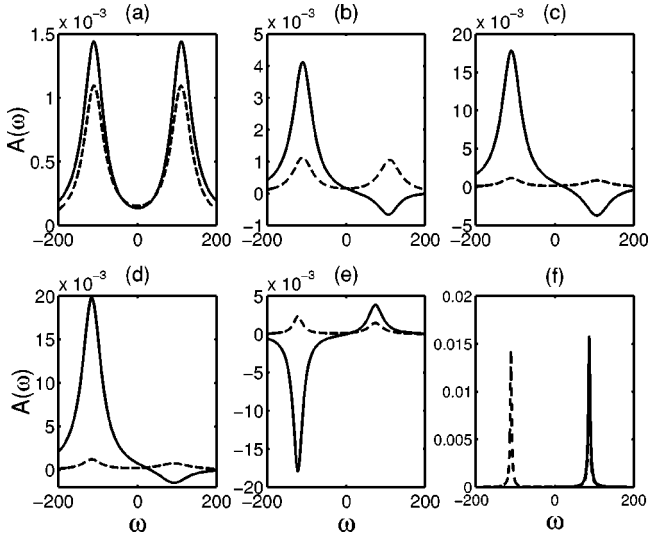

FIG. 3. Same as Fig.1, but with $\omega_{21}=200$ and $N=20$.

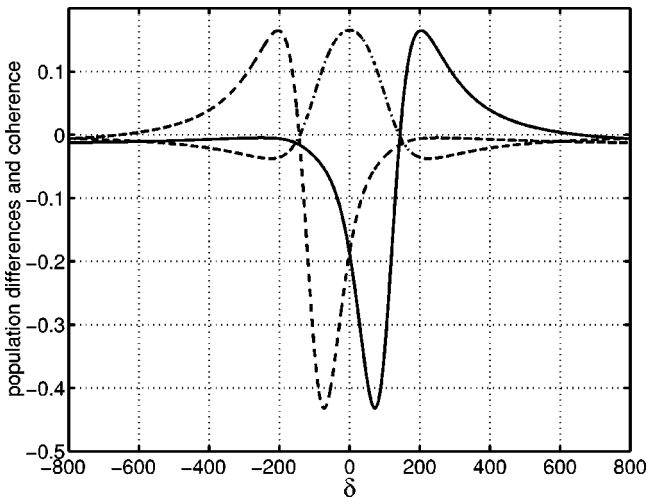

FIG. 4. The steady-state population differences and coherence vs the cavity detuning, for $g_1=g_2=10$, $\omega_{21}=200$, $N=20$, and $\eta=1$. The solid, dashed, and dot-dashed lines respectively represent $(\langle A_{11}\rangle-\langle A_{00}\rangle)$, $(\langle A_{22}\rangle-\langle A_{00}\rangle)$, and $\mathrm{Re}(\langle A_{12}\rangle)$.

$|0\rangle \leftrightarrow |2\rangle$. The gain at each sideband has a different origin. To show this, we first plot the steady-state population differences between the excited sublevels and the ground level, $\langle A_{11}\rangle-\langle A_{00}\rangle$ and $\langle A_{22}\rangle-\langle A_{00}\rangle$, and the coherence between the excited sublevels, $\langle A_{12}\rangle$, against the cavity detuning δ in Fig. 4 for $g_1=g_2=10$, $\kappa=100$, $\omega_{21}=200$, and $N=20$. It is clear that the steady-state populations and coherence are highly dependent on the cavity frequency. The coherence is symmetric with the cavity detuning and reaches its maximum value at $\delta=0$, while the population differences are asymmetric. Furthermore, population inversion may be achieved for certain cavity frequencies, for example, if $143.8<\delta<650$, then $\langle A_{11}\rangle-\langle A_{00}\rangle>0$, while $\langle A_{22}\rangle>\langle A_{00}\rangle$ in the region $-650<\delta<-143.8$. Therefore, the gain in the region of $-143.8<\delta<143.8$ must stem from the cavity-induced steady-state coherence between the two dipole-forbidden excited sublevels, rather than from the population inversion between the two dipole transition levels. However, population inversions may result in probe gain when the cavity detuning is in the regions $-650<\delta<-143.8$ and $143.8<\delta<650$. We thus conclude that, in the case of $\delta>0$, as shown in Figs. 1–3, the gain at the lower frequency sideband comes from the contribution of the steady-state atomic coherence $\langle A_{12}\rangle$, while the gain at the other sideband is attributed to the steady-state population inversion $(\langle A_{11}\rangle>\langle A_{00}\rangle)$.

Noting that, in the absence of interference ($\eta=0$), the quantities $\langle A_{11}\rangle=\langle A_{22}\rangle=N/(3N+1)$, $\langle A_{00}\rangle=(N+1)/(3N+1)$, and $\langle A_{12}\rangle=0$ are independent of the cavity detuning, the cavity frequency dependence of the steady-state populations and coherence is a manifestation of cavity-induced quantum interference.

To further explore the origin of the probe gain, we separate the Autler-Townes spectrum into two parts, in which one corresponds to the contribution of the populations, while the other results from the coherence, in Fig. 5, for $g_1=g_2=10$, $\kappa=100$, $\omega_{21}=200$, $N=20$, and various cavity fre-

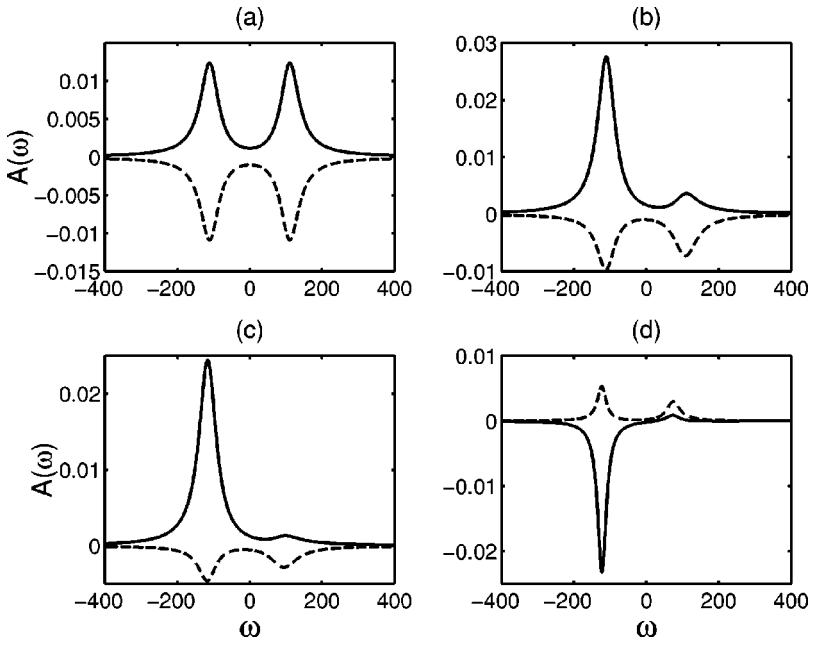

FIG. 5. Different contributions to the absorption spectrum, for $g_1=g_2=10$, $\kappa=100$, $\omega_{21}=200$, $N=20$, $\eta=1$, and $\delta=0$, 50, 100, 200 in (a)–(d), respectively. The solid curves represent the contributions of the population differences, while the dashed curves are those of the coherences.

quencies. It is obvious that when $\delta=0$, 50, and 100 the contributions of the coherence to the spectrum are negative (i.e., probe gain), whereas the populations make positive contributions; see, for example, Figs. 5(a)–5(c). One can also see that the spectral component resulting from the populations is symmetric only when $\delta=0$; otherwise, it has different values at the lower and higher frequency sidebands, which are proportional to $(\langle A_{00}\rangle-\langle A_{11}\rangle)$ and $(\langle A_{00}\rangle-\langle A_{22}\rangle)$, respectively. As shown in Fig. 4, if the cavity detuning is zero, then $(\langle A_{00}\rangle-\langle A_{11}\rangle)=(\langle A_{00}\rangle-\langle A_{22}\rangle)$, whereas $(\langle A_{00}\rangle-\langle A_{11}\rangle)>(\langle A_{00}\rangle-\langle A_{22}\rangle)$ for $\delta=50$ and 100. As a result, the lower frequency peak is higher than the other in the cases $\delta=50$ and $\delta=100$. The total spectrum may therefore exhibit probe gain at the higher frequency sideband at these cavity frequencies. See for example, Figs. 3(c) and 3(d). The gain is purely attributable to the cavity-induced steady-state atomic coherence. However, when $\delta=200$, the situation is reversed: the coherence gives rise to probe absorption, while the populations lead to gain at the lower frequency sideband, due to population inversion between the levels $|0\rangle$ and $|1\rangle$, as illustrated in Fig. 4.

In summary, we have shown that maximal quantum interference can be achieved in a V-type atom coupled to a single-mode, frequency-tunable cavity field at a finite temperature, with a preselected polarization in the bad cavity limit. There are no special restrictions on the atomic dipole moments, as long as the polarization of the cavity field is preselected. We have investigated the cavity modification of the Autler-Townes spectrum of this system, and predicted probe gain at either sideband of the doublet, depending upon the cavity resonant frequency, when the excited sublevel splitting is very large (of the same order as the cavity linewidth) and the mean number of thermal photons greatly exceeds unity. The gain occurring at different sidebands has different origins: for $\delta>0$, the lower frequency gain is due to the nonzero steady-state coherence, while the higher frequency gain is attributed to the steady-state population inversion. Both the nonzero coherence and the population inversion originate from cavity-induced quantum interference. It is also possible to choose the detuning so that one of the Autler-Townes sidebands is suppressed.

This work was supported by the United Kingdom EPSRC. We gratefully acknowledge conversations with Z. Ficek. We would also like to thank S. Menon for bringing Ref. [20] to our attention.

[1] E. Arimondo, in *Progress in Optics* (North Holland, Amsterdam, 1996), p. 257; M.O. Scully and S.Y. Zhu, Science **281**, 1973 (1998).

[2] S.E. Harris, Phys. Rev. Lett. **62**, 1033 (1989); S.E. Harris and J.J. Macklin, Phys. Rev. A **40**, R4135 (1989); A. Imamoglu, *ibid.* **40**, R2835 (1989).

[3] K.J. Boller, A. Imamoglu, and S.E. Harris, Phys. Rev. Lett. **66**, 2593 (1991).

[4] M.O. Scully, Phys. Rev. Lett. **67**, 1855 (1991).

[5] D.A. Cardimona, M.G. Raymer, and C.R. Stroud, Jr., J. Phys. B **15**, 65 (1982); G.C. Hegerfeldt and M.B. Plenio, Phys. Rev. A **46**, 373 (1992).

[6] P. Zhou and S. Swain, Phys. Rev. Lett. **77**, 3995 (1996); Phys. Rev. A **56**, 3011 (1997).

[7] S.Y. Zhu and M.O. Scully, Phys. Rev. Lett. **76**, 388 (1996); H. Lee, P. Polynkin, M.O. Scully, and S.-Y. Zhu, Phys. Rev. A **55**, 4454 (1997); E. Paspalakis and P.L. Knight, Phys. Rev. Lett. **81**, 293 (1998).

[8] H.R. Xia, C.Y. Ye, and S.Y. Zhu, Phys. Rev. Lett. **77**, 1032 (1996).

[9] C.H. Keitel, Phys. Rev. Lett. **83**, 1307 (1999).
[10] P. Zhou and S. Swain, Phys. Rev. Lett. **78**, 832 (1997); J. Opt. Soc. Am. B **15**, 2583 (1998).
[11] E. Paspalakis, N.J. Kylstra, and P.L. Knight, Phys. Rev. Lett. **82**, 2079 (1999).
[12] P.R. Berman, Phys. Rev. A **58**, 4886 (1998).
[13] L. Li, X. Wang, J. Wang, G. Lazarov, J. Qi, and A.M. Lyyra, Phys. Rev. Lett. **84**, 4016 (2000).
[14] J. Wang, H.M. Wiseman, and Z. Ficek, Phys. Rev. A **62**, 013818 (2000).
[15] M.O. Scully, S.Y. Zhu, and A. Gavrielides, Phys. Rev. Lett. **62**, 2813 (1989); M. Fleischauer, C.H. Keitel, L.M. Narducci, M.O. Scully, S.Y. Zhu, and M.S. Zubairy, Opt. Commun. **94**, 599 (1992); S.Y. Zhu, L.M. Narducci, and M.O. Scully, Phys. Rev. A **52**, 4791 (1995); G.S. Agarwal, *ibid.* **54**, R3734 (1996); E. Paspalakis, C.H. Keitel, and P.L. Knight, *ibid.* **58**, 4868 (1998).
[16] H.R. Gray, R.M. Whitely, and C.R. Stroud, Jr., Opt. Lett. **3**, 218 (1978); G. Orriols, Nuovo Cimento B **53**, 1 (1979); R.P. Hackel and S. Ezekiel, Phys. Rev. Lett. **42**, 1736 (1979); M. Kaivola, P. Thorsen, and O. Poulsen, Phys. Rev. A **32**, 207 (1985); K. Hakuta, L. Marmet, and B.P. Stoicheff, Phys. Rev. Lett. **66**, 596 (1991); J.E. Field, K.H. Hahn, and S.E. Harris, *ibid.* **67**, 3062 (1991); A. Kasapi, M. Jain, G.Y. Yin, and S.E. Harris, Phys. Rev. Lett. **74**, 2447 (1995); M. Xiao, Y. Li, S. Jin, and J. Gea-Banacloche, Phys. Rev. Lett. **74**, 666 (1995); Y. Li and M. Xiao, Phys. Rev. A **51**, R2703 (1995); **51**, 4959 (1995); R.R. Moseley, S. Shepherd, D.J. Fulton, B.D. Sinclair, and M.H. Dunn, Phys. Rev. Lett. **74**, 670 (1995).
[17] A.K. Patnaik and G.S. Agarwal, Phys. Rev. A **59**, 3015 (1999).
[18] G.S. Agarwal, Phys. Rev. Lett. **84**, 5500 (2000).
[19] P. Zhou and S. Swain, Opt. Commun. **179**, 267 (2000).
[20] S. Menon and G.S. Agarwal, Phys. Rev. A **61**, 013807 (2000).
[21] G.S. Agarwal, W. Lange, and H. Walther, Phys. Rev. A **48**, 4555 (1993); P. Zhou and S. Swain, *ibid.* **58**, 1515 (1998), and references therein.